



HAL
open science

Hydride-encapsulated bimetallic clusters supported by 1,1-dithiolates

Yu-Jie Zhong, Jian-Hong Liao, Tzu-Hao Chiu, Ying-Yann Wu, Samia Kahlal,
Jean-Yves Saillard, C.W. Liu

► **To cite this version:**

Yu-Jie Zhong, Jian-Hong Liao, Tzu-Hao Chiu, Ying-Yann Wu, Samia Kahlal, et al.. Hydride-encapsulated bimetallic clusters supported by 1,1-dithiolates. *Chemical Communications*, 2020, 56 (65), pp.9300-9303. 10.1039/d0cc03848b . hal-02928949

HAL Id: hal-02928949

<https://hal.science/hal-02928949>

Submitted on 9 Nov 2020

HAL is a multi-disciplinary open access archive for the deposit and dissemination of scientific research documents, whether they are published or not. The documents may come from teaching and research institutions in France or abroad, or from public or private research centers.

L'archive ouverte pluridisciplinaire **HAL**, est destinée au dépôt et à la diffusion de documents scientifiques de niveau recherche, publiés ou non, émanant des établissements d'enseignement et de recherche français ou étrangers, des laboratoires publics ou privés.

Hydride-Encapsulated Bimetallic Clusters Supported by 1, 1-Dithiolates

Yu-Jie Zhong,^a Jian-Hong Liao,^a Tzu-Hao Chiu,^a Ying-Yann Wu,^b Samia Kahlal,^c Jean-Yves Saillard^c and C. W. Liu*^a

^a Department of Chemistry, National Dong Hwa University, Hualien 974301, Taiwan (R. O. C.). E-mail: chenwei@mail.ndhu.edu.tw

^b Institute of Chemistry, Academia Sinica, Taipei 11528, Taiwan (R. O. C.)

^c Univ Rennes, CNRS, ISCR-UMR 6226, F-35000 Rennes, France.

DOI: 10.1039/D0CC03848B

Two mixed-metal hydride clusters, corresponding to $x = 3$ and 4 , were structurally characterized from a set of atomically precise heptanuclear clusters, $\text{Cu}_x\text{Ag}_{7-x}(\text{H})\{\text{S}_2\text{P}(\text{O}^i\text{Pr})_2\}_6$ ($x = 1-6$). An interstitial hydride lying at the center of a tricapped tetrahedral cage was located and refined anisotropically by using X-ray data, and its presence ascertained by multinuclear NMR spectroscopy and DFT calculations.

Metal hydrides are known for their glamorous structural diversity and bonding features,¹ as well as their potential applications in hydrogen storage² and various catalytic processes.³ The search for new Cu/Ag hydrido nanoclusters (NCs) is emerging and topical.^{4,5-20} Several high-nuclearity Cu(I)/Ag(I) hydrides, $[\text{Cu}_{25}\text{H}_{10}(\text{SPhCl}_2)_{18}]^{3-}$,⁵ $[\text{Cu}_{16}\text{H}_{14}(\text{D}^2\text{-dpmpm})_4]^{2+}$,⁶ $[\text{Cu}_{18}\text{H}_{17}(\text{PPh}_3)_{10}]^{+}$,⁷ and $[\text{Ag}_{10}\text{H}_8(\text{dppa})_6]^{2+}$,⁸ have been reported. A few polyhydrido NCs displaying M(I)/M'(O) character also exist, such as the 2e species $[\text{Cu}_{25}\text{H}_{22}(\text{PPh}_3)_{12}]^{+}$,⁷ $[\text{Cu}_{29}\text{Cl}_4\text{H}_{22}(\text{Ph}_2\text{phen})_{12}]^{+}$,⁹ $[\text{Cu}_{61}(\text{S}^t\text{Bu})_{26}\text{S}_6\text{Cl}_6\text{H}_{14}]^{+}$,¹⁰ and $[\text{Ag}_{40}(\text{DMBT})_{24}(\text{PPh}_3)_8\text{H}_{12}]^{2+}$.¹¹ A pitfall in the structural characterization of these NCs is that the position of the hydrides cannot be accurately determined from X-ray diffraction alone. Nevertheless, the molecular formulation can be determined by the spectroscopic evidences of ESI-MS, multinuclear NMR, in combination with DFT calculations. Our group has isolated and structurally characterized a series of tetracapped-tetrahedral octanuclear¹² and tricapped-tetrahedral heptanuclear clusters¹³ encapsulating a tetrahedrally coordinated hydride, the position of which was fully established by neutron diffraction on the compound $[\text{Cu}_7(\text{H})\{\text{S}_2\text{C}(\text{aza-15-crown-5})_6\}]^{13b}$. Later, Cu(I) polyhydrides $[\text{Cu}_{28}(\text{H})_{15}\{\text{S}_2\text{CN}(\text{Pr})_2\}_{12}](\text{PF}_6)$,¹⁴ $[\text{Cu}_{20}(\text{H})_{11}\{\text{E}_2\text{P}(\text{O}^i\text{Pr})_2\}_9]$ ($\text{E} = \text{S},^{15} \text{Se}^{16}$), $[\text{Cu}_{30}(\text{H})_{18}\{\text{E}_2\text{P}(\text{OR})_2\}_{12}]$ ($\text{E} = \text{S}, \text{Se}$; $\text{R} = \text{Pr}, \text{Pr}, \text{Bu}$),¹⁷ $[\text{Cu}_{32}(\text{H})_{20}\{\text{S}_2\text{P}(\text{O}^i\text{Pr})_2\}_{12}]$,¹⁸ $[\text{Cu}_{11}(\text{H})_2\{\text{S}_2\text{P}(\text{O}^i\text{Pr})_2\}_6(\text{C}_2\text{Ph})_3]$,¹⁹ and the Cu(I)/Pd(O) hydrides, $[\text{Pd@Cu}_{14}(\text{H})_2\{\text{S}_2\text{CN}(\text{Pr})_2\}_6(\text{C}_2\text{Ph})_6]$,²⁰ were structurally characterized by both single-crystal X-ray and neutron diffraction, from which a new synthetic concept has been established, based on the fact that hydride additions assist the growth of nanoscale copper clusters.^{4a}

Although neutron diffraction is the most reliable technique to locate hydrogen atoms, it is not conveniently available. In addition, the successful performance of a neutron diffraction experiment is not an easy task, and the following points must be overcome: (i) Grow single crystals of sufficiently big size as well as high quality; (ii) Avoid high background noise especially for compounds containing a large number of H atoms. In comparison with neutron experiments, in-house X-ray diffraction rapidly provides results for further analysis. Grabowsky's group applied the Hirshfeld atom refinement (HAR) method to refine hydrogen with aspherical scattering factors in X-ray data.²¹ However, the HAR method is mostly applied for organic compounds, but rarely for inorganic cluster compounds.

Mixed-metal hydride clusters are emergingly challenging in this field. Not only will one encounter the unavoidable disorder issues on metal sites, but also face the high probability of co-crystallization from their reaction mixtures. In our previous computational investigations on the octanuclear species $[\text{M}_8(\text{H})\text{L}_6]^+$ ($\text{M} = \text{Cu}, \text{Ag}$; $\text{L} = \text{dithio- or diselenolate}$), the metal framework was found to exhibit a tetracapped-tetrahedral geometry of which each metal site can be either Cu(I) or Ag(I).^{12f} The related $\text{M}_7(\text{H})\text{L}_6$ can be obtained from further reduction of $[\text{M}_8(\text{H})\text{L}_6]^+$ to form a tricapped-tetrahedral metal framework.¹³ These results inspired us to synthesize mixed-metal hydride clusters. Herein we report an one-pot synthesis and characterizations of $\text{Cu}_x\text{Ag}_{7-x}(\text{H})\{\text{S}_2\text{P}(\text{O}^i\text{Pr})_2\}_6$, $x = 1-6$ (abbreviated as $\text{Cu}_x\text{Ag}_{7-x}\text{H}$). Surprisingly it is our first successful attempt on performing anisotropic refinement of an interstitial hydride by using X-ray diffraction data.

The synthesis was performed with $[\text{Ag}(\text{CH}_3\text{CN})_4]\text{PF}_6$, $[\text{Cu}(\text{CH}_3\text{CN})_4]\text{PF}_6$, and $\text{NH}_4[\text{S}_2\text{P}(\text{O}^i\text{Pr})_2]$ dissolved in THF solution first followed by adding NaBH_4 as a hydride provider. The final products were purified by column chromatography to yield $\text{Cu}_x\text{Ag}_{7-x}(\text{H})\{\text{S}_2\text{P}(\text{O}^i\text{Pr})_2\}_6$, $x = 1-6$. Two crystals grown from the mixtures were hand-picked to collect diffraction data. The crystal structure of the first one turned out to have one metal site (M_{top}) statistically occupied by 50% Cu and 50% Ag, thus corresponding to a co-crystallized product of composition $[\text{Cu}_3\text{Ag}_4(\text{H})\{\text{S}_2\text{P}(\text{O}^i\text{Pr})_2\}_6]_{0.5}[\text{Cu}_4\text{Ag}_3(\text{H})\{\text{S}_2\text{P}(\text{O}^i\text{Pr})_2\}_6]_{0.5}$ (**1**). Intriguingly, the composition of the second crystal is $\text{Cu}_4\text{Ag}_3(\text{H})\{\text{S}_2\text{P}(\text{O}^i\text{Pr})_2\}_6$ (**2**). In the crystal structure of **1**, the seven metal atoms constitute a tricapped-tetrahedral framework, $(\mu_3\text{-Cu})_3(\text{M}_{\text{top}}\text{Ag}_3)$ ($\text{M}_{\text{top}} = \text{Cu}_{0.5}\text{Ag}_{0.5}$), of ideal C_{3v} symmetry, with the encapsulated hydride lying at the center of the $\text{M}_{\text{top}}\text{Ag}_3$ tetrahedron. The entire metal core is stabilized by six diisopropyl dithiophosphate (dtp) ligands, reducing the whole molecular symmetry to C_3 . The 3-fold rotational axis passes through M_{top} , the central hydride and the middle of the $(\text{Ag}_{\text{tri}})_3$ triangular face of the inner tetrahedron (Figure 1a). Unlike in **1**, the M_{top} position in structure **2** is fully occupied by a Cu atom (Figure 1b). *It is worthwhile to mention that the encapsulated H-atom revealed in both **1** and **2**, is the first reported example of a hydride bonded to both Cu and Ag atoms.*

Selected bond lengths are listed in Table S1. The distances between metal atoms in **1** and **2** are almost identical. Small differences exist in $\text{M}_{\text{top}}\text{-M}_{\text{tri}}$ (3.0890(3)-3.2531(3) Å in **1**; 3.0970(5)-3.2543(5) Å in **2**), $\text{M}_{\text{cap}}\text{-M}_{\text{top}}$ (2.7368(4)-2.7499(4) Å in **1**;

2.7152(6)-2.7312(6) Å in **2**), and $M_{\text{cap}}-M_{\text{tri}}$ (2.9208(3) - 3.0324(4) Å in **1**; 2.8950(5) - 3.0118(6) Å in **2**). The $M_{\text{top}}(\text{Ag}_{\text{tri}})_3$ tetrahedron in **1** can be compared to its analog in $[\text{Ag}_7(\text{H})\{\text{S}_2\text{CC}(\text{CN})_2\}_6]^{6-}$, **3**, which metal framework also reveals a tricapped-tetrahedral geometry, but with an elongated inner tetrahedron (Figure 1c). The $M_{\text{top}}-M_{\text{tri}}$ distances of the latter are much longer than those in **1** and **2** (Table S1). The S...S bite distance in **3**, which is approximately 0.35-0.43 Å shorter than in **1** and **2**, could be the explanation for this elongated tetrahedron. The H- M_{top} distances are 1.65(2) Å in **2** and 1.83(4) Å in **1**. The angles of $M_{\text{top}}-H-M_{\text{tri}}$ and $M_{\text{tri}}-H-M_{\text{tri}}$ in **1(2)** are 109(2)-118(2)° (117.6(5)-124.3(5)°) and 100(2)-105(2)° (96.3(4)-97.7(4)°). In fact the tetrahedral coordination of the hydride observed in both **1** and **2** is one among several possible four-coordinated hydride configurations such as in square-planar,¹⁵ elongated tetrahedral,^{13a-b} distorted seesaw,¹⁷ and trigonal pyramidal modes.¹⁹

The hydride atom in both **1** and **2** was located from the Fourier density map. It was initially refined isotropically without any constraints in data **1**. To our great surprise, a further anisotropic refinement of the hydride using the X-ray data of **1** was successful. In general, such anisotropic refinement usually results in non-positive-definite in hydrogen refinement, because H has only one electron. It is highly correlated to the crystal orientation during the entire data collection. However, the prediction to collect informative reflections related to hydride is extremely difficult. One should ensure that the coverage of the data collection is as high as possible so that more dataset can be incorporated in order to increase the redundancy, and the most important thing is that a low-temperature experiment should be performed to reduce the temperature effect. The data analysis demonstrated that those of **1** have higher resolution ($d \sim 0.73$ Å) and redundancy (4.15) than those of **2** ($d \sim 0.78$ Å, redundancy 3.17). It can only be assumed that more informative reflections were collected in the data of **1**. Sum of the above reasons, the hydride in **1** could be anisotropically refined to convergence with unexpected success. It is of note that the hydrides in $[\text{CuHP}(\text{NMe}_2)_3]_6$ were located and refined by using X-ray data collected at -162 °C.²²

DFT calculations²³ on two simplified C_3 models for the clusters present in **1** and **2**, namely $[\text{Cu}_3\text{Ag}_4(\text{H})\{\text{S}_2\text{PH}_2\}_6]$ (**1'**) and $[\text{Cu}_4\text{Ag}_3(\text{H})\{\text{S}_2\text{PH}_2\}_6]$ (**2'**) reproduce nicely their structures (Table S1). The building of C_3 isomers of **1'** and **2'** in which the three M_{cap} atoms are Ag (in the place of Cu), destabilizes the systems by 13.6 and 16.4 kcal/mol, (free energy) respectively. Obviously, Cu prefers capping positions. This is also exemplified by calculations on the tetracapped-tetrahedral octanuclear model $[\text{Cu}_4\text{Ag}_4(\text{H})\{\text{S}_2\text{PH}_2\}_6]$ for which the $\text{H}@\text{Ag}_4@\text{Cu}_4$ isomer is found more stable than its $\text{H}@\text{Cu}_4@\text{Ag}_4$ relative by 6.0 kcal/mol. Exchanging M_{top} with one M_{tri} in **2'** destabilizes the cluster by 2.6 kcal/mol, indicating that among the four inner tetrahedral positions, Cu prefers the M_{top} one. The $M_{\text{cap}} > M_{\text{top}} > M_{\text{tri}}$ site preference for Cu is related for its strong affinity to bind sulphur (M_{cap} : sulphur only) and its stronger than Ag binding to hydride ($M_{\text{top}}-H$ stronger than $M_{\text{tri}}-H$).

Due to the intrinsic characters of highly similar polarities, the products, $\text{Cu}_x\text{Ag}_{7-x}(\text{H})\{\text{S}_2\text{P}(\text{O}^i\text{Pr})_2\}_6$, $x = 1-6$, cannot be further separated. While the reactions were performed with various stoichiometric ratios $\text{Cu}:\text{Ag}:\text{L}:\text{H} = x:(7-x):6:1$, ($x = 1-6$), the resulting products based on their ¹H NMR spectra are very similar. The hydride resonance displays in a wide distribution (4.9 - 6.3 ppm) that integrates to one H relative to 12 methylene and 72 methyl protons of a total of six di-isopropyl dithiophosphate ligands (Figure 2). The resonance centered at 5.0 ppm splits into a doublet of doublets ($^1J_{1\text{H}-107\text{Ag}} = 86.7$ Hz, $^1J_{1\text{H}-109\text{Ag}} = 99.7$ Hz), which is due to the hydride coupled with different isotopomers, ¹⁰⁷Ag and ¹⁰⁹Ag nuclei. This doublet of doublets peak can be assigned to the Cu_6AgH compound. Based on the same principle, the resonance centered at 5.44 ppm with a triplet of triplets pattern can be assigned to $\text{Cu}_5\text{Ag}_2\text{H}$. It clearly suggests that the hydride coupled with two pretend, magnetically equivalent silver nuclei, and the distribution of the splitting pattern is the superposition of the spectra of the different isotopomers. It is confirmed by the simulated pattern of $M_xM'^{2-x}\text{H}$ (M , ¹⁰⁷Ag; M' , ¹⁰⁹Ag) spin system (Figure 3) with the assumed coupling constant of $^1J_{1\text{H}-107\text{Ag}}$ (65.0 Hz) and $^1J_{1\text{H}-109\text{Ag}}$ (74.7 Hz). The resonance in the range of 5.9 - 6.4 ppm displays a mixture combination that can be resolved as $\text{Cu}_4\text{Ag}_3\text{H}$ (quartet of quartets), $\text{Ag}_4\text{Cu}_3\text{H}$ (quintet of quintets), $\text{Cu}_2\text{Ag}_5\text{H}$ (sextet of sextets), and CuAg_6H (septet of septets), respectively. Their simulated spectra are stacked in Figure 3. The sum of all spectra (red) exactly matches with the experimental one (inset of Figure 2). An observed doublet resonance at 1080.5 ppm ($^1J_{1\text{H}-109\text{Ag}} = 74.5$ Hz) in ¹⁰⁹Ag NMR spectrum (Figure S1) matches with $^1J_{1\text{H}-109\text{Ag}}$ (74.7 Hz) of $\text{Cu}_5\text{Ag}_2\text{H}$ in the ¹H NMR spectrum. Only $\text{Cu}_5\text{Ag}_2\text{H}$, $\text{Cu}_4\text{Ag}_3\text{H}$, $\text{Cu}_3\text{Ag}_4\text{H}$, and $\text{Cu}_2\text{Ag}_5\text{H}$ species could be observed. The other compounds were not detected due to lower quantities. The corresponding chemical shifts and coupling constants are listed in Table 1. $\text{Cu}_4\text{Ag}_3\text{H}$ shows the most intense peak in both ¹H, ²H (Figure S8), and ¹⁰⁹Ag NMR spectra, which is highly correlated with the crystal data. Variable-temperature ¹H NMR experiment was performed (Figure S2). The hydride resonances are all slightly upfielded by ~ 0.15 ppm at -60 °C. Their lineshapes did not change upon temperature decreases to -40 °C, then became broad at -60 °C. The NMR spectroscopic data suggests that fast intrachanges between capping and inner vertices atoms occur at the NMR time scale. Besides, the coupling constant ($^1J_{\text{HAg}}$) of each compound in the $\text{Cu}_x\text{Ag}_{7-x}\text{H}$ mixture was discernible. Presumably the metal exchange tends to be intramolecular rather than intermolecular and such a fluxional behavior has been observed in the $\text{Ag}_7(\text{H})\text{L}_6$ analogs ($\text{L} = [\text{S}_2\text{CC}(\text{CN})_2]^{2-}$, $[\text{E}_2\text{P}(\text{OR})_2]^-$ E = S, Se).^{13a,c}

ESI-MS spectrum displayed a wide distribution of $\text{Cu}_x\text{Ag}_{7-x}\text{H}$ ($x = 0 - 7$). The most and second intense peaks at m/z 2000.3582 and 2044.3331 correspond to the molecular ion $[\text{Cu}_4\text{Ag}_3(\text{H})\{\text{S}_2\text{P}(\text{O}^i\text{Pr})_2\}_6 + \text{Ag}^+ + 2(\text{H}_2\text{O})]^+$ (calcd. m/z 2000.4689) and $[\text{Cu}_3\text{Ag}_4(\text{H})\{\text{S}_2\text{P}(\text{O}^i\text{Pr})_2\}_6 + \text{Ag}^+ + 2(\text{H}_2\text{O})]^+$ (calcd. m/z 2044.4444), respectively (Figure S4). Interestingly, both $[\text{Cu}_7(\text{H})\{\text{S}_2\text{P}(\text{O}^i\text{Pr})_2\}_6 + \text{Ag}^+ + 2(\text{H}_2\text{O})]^+$ and $[\text{Ag}_7(\text{H})\{\text{S}_2\text{P}(\text{O}^i\text{Pr})_2\}_6 + \text{Ag}^+ + 2(\text{H}_2\text{O})]^+$ can be barely seen (Figure S5). It is noted that both $\text{Cu}_x\text{Ag}_{7-x}(\text{H})\{\text{S}_2\text{P}(\text{O}^i\text{Pr})_2\}_6$ ($x = 0$ and 7) species were not observed in the ¹H NMR spectrum. This can be attributed to rearrangement reactions taking place in the gas phase.

Calculations on models of the non-structurally characterized clusters, *i.e.* $\text{Cu}_x\text{Ag}_{7-x}(\text{H})\{\text{S}_2\text{PH}_2\}_6$ ($x = 1, 2, 5, 6$), indicate that their isomers of lowest energy follow the metal site preference rule discussed above (Figure S7). Their computed ¹H NMR hydride chemical shifts display the best agreement with their experimental counterparts (Table 1).

In conclusion, a set of mixed-metal hydride compounds $\text{Cu}_x\text{Ag}_{7-x}(\text{H})\{\text{S}_2\text{P}(\text{O}^i\text{Pr})_2\}_6$ ($x = 1-6$) have been synthesized and

characterized by multi-nuclear NMR, ESI mass spectroscopy, DFT simulation and both Cu₃Ag₄H and Cu₄Ag₃H by single-crystal X-ray diffraction. An unprecedented (μ_4 -H) hydride encapsulated in a hetero-metallic M₄ (Ag₃Cu) tetrahedral cage, which can be refined anisotropically in crystal **1**, is reported. It is expected that the addition of a supplementary Cu(I)/Ag(I) capping metal such as Cu(I)/Ag(I) would lead to a stable octanuclear species since there is one empty site along the C₃ axis.

Conflicts of interest

There are no conflicts to declare.

Acknowledgements

This work was supported by the Ministry of Science and Technology of Taiwan (109-2113-M-259-008) and the GENCI French national computer resource center (project A0050807367). We thank Academia Sinica High-Field NMR Center (HFNMRC) for technical support; HFNMRC is funded by Academia Sinica Core Facility and Innovative Instrument Project (AS-CFII-108-112).

Notes and references

- (a) R. Poli, M. Peruzzini, *Recent Advances in Hydride Chemistry*; Amsterdam, 2001; p 557; (b) Z. Lin, M. B. Hall, *Coord. Chem. Rev.*, 1994, **135**, 845-879; (c) F. Maseras, A. Lledos, E. Clot, O. Eisenstein, *Chem. Rev.*, 2000, **100**, 601-636; (d) A. J. Hoskin, D. W. Stephan, *Coord. Chem. Rev.*, 2002, **233–234**, 107-129; (e) F. Gloaguen, T. B. Rauchfuss, *Chem. Soc. Rev.*, 2009, **38**, 100-108.
- (a) B. Sakintuna, F. Lamari-Dakrim, M. Hirscher, *Int. J. Hydrog. Energy*, 2007, **32**, 1121-1140; (b) L. Schlapbach, A. Züttel, *Nature*, 2001, **414**, 353-358; (c) R. S. Dhayal, W. E. van Zyl, C. W. Liu, *Dalton Trans.*, 2019, **48**, 3531-3538.
- (a) R. J. Angelici, *Acc. Chem. Res.*, 1988, **21**, 387-394; (b) D. M. Brestensky, J. M. Stryker, *Tetrahedron Lett.*, 1989, **30**, 5677-5680; (c) K. M. Miller, T. Luanphaisarnnont, C. Molinaro, T. F. Jamison, *J. Am. Chem. Soc.*, 2004, **126**, 4130-4131; (d) S. K. Brayshaw, A. Harrison, J. S. McIndoe, F. Marken, P. R. Raithby, J. E. Warren, A. S. Weller, *J. Am. Chem. Soc.*, 2007, **129**, 1793-1804; (e) Q. Tang, Y. Lee, D.-Y. Li, W. Choi, C. W. Liu, D. Lee, D.-e. Jiang, *J. Am. Chem. Soc.*, 2017, **139**, 9728-9736.
- (a) R. S. Dhayal, W. E. van Zyl, C. W. Liu, *Acc. Chem. Res.*, 2016, **49**, 86-95; (b) A. J. Jordan, G. Ialic, J. P. Sadighi, *Chem. Rev.*, 2016, **116**, 8318-8372; (c) T. Nakajima, K. Nakamae, Y. Ura, T. Tanase, *Eur. J. Inorg. Chem.*, **2020**, 2211-2226; (d) T. Nakajima, T. Tanase, *Chem. Lett.* 2020, **49**, 386-394.
- C. Sun, N. Mammen, S. Kaappa, P. Yuan, G. Deng, C. Zhao, J. Yan, S. Malola, K. Honkala, H. Häkkinen, B. K. Teo, N. Zheng, *ACS Nano.*, 2019, **13**, 5975-5986.
- K. Nakamae, T. Nakajima, Y. Ura, Y. Kitagawa, T. Tanase, *Angew. Chem. Int. Ed.*, 2019, **59**, 2262-2267.
- T.-A. D. Nguyen, Z. R. Jones, B. R. Goldsmith, W. R. Buratto, G. Wu, S. L. Scott, T. W. Hayton, *J. Am. Chem. Soc.*, 2015, **137**, 13319-13324.
- H. Z. Ma, A. I. McKay, A. Mravak, M. S. Scholz, J. M. White, R. J. Mulder, E. J. Bieske, V. Bonačić-Koutecky, R. A. J. O'Hair, *Nanoscale*, 2019, **11**, 22880-22889.
- T.-A. D. Nguyen, Z. R. Jones, D. F. Leto, G. Wu, S. L. Scott, T. W. Hayton, *Chem. Mater.*, 2016, **28**, 8385-8390.
- A. Ghosh, R.-W. Huang, B. Alamer, E. Abou-Hamad, M. N. Hedhili, O. F. Mohammed, O. M. Bakr, *ACS Materials Lett.*, 2019, **1**, 297-302.
- X. Yuan, C. Sun, X. Li, S. Malola, B. K. Teo, H. Häkkinen, L.-S. Zheng, N. Zheng, *J. Am. Chem. Soc.*, 2019, **141**, 11905-11908.
- (a) C. W. Liu, B. Sarkar, Y.-J. Huang, P.-K. Liao, J.-C. Wang, J.-Y. Saillard, S. Kahlal, *J. Am. Chem. Soc.*, 2009, **131**, 11222-11233; (b) P.-K. Liao, D.-R. Shi, J.-H. Liao, C. W. Liu, A. V. Artem'ev, V. A. Kuimov, N. K. Gusarova, B. A. Trofimov, *Eur. J. Inorg. Chem.*, 2012, 4921-4929; (c) P.-K. Liao, B. Sarkar, H.-W. Chang, J.-C. Wang, C. W. Liu, *Inorg. Chem.*, 2009, **48**, 4089-4097; (d) C. W. Liu, H.-W. Chang, C.-S. Fang, B. Sarkar, J.-C. Wang, *Chem. Commun.*, 2010, **46**, 4571-4573; (e) C. W. Liu, H.-W. Chang, B. Sarkar, J.-Y. Saillard, S. Kahlal, Y.-Y. Wu, *Inorg. Chem.*, 2010, **49**, 468-475; (f) C. Latouche, S. Kahlal, E. Furet, P.-K. Liao, Y.-R. Lin, C.-S. Fang, J. Cury, C. W. Liu, J.-Y. Saillard, *Inorg. Chem.*, 2013, **52**, 7752-7765; (g) P.-K. Liao, K.-G. Liu, C.-S. Fang, C. W. Liu, J. P. Fackler, Jr. Y.-Y. Wu, *Inorg. Chem.*, 2011, **50**, 8410-8417.
- (a) P.-K. Liao, K.-G. Liu, C.-S. Fang, Y.-Y. Wu, C. W. Liu, *J. Clust. Sci.*, 2019, **30**, 1185-1193; (b) P.-K. Liao, C.-S. Fang, A. J. Edwards, S. Kahlal, J.-Y. Saillard, C. W. Liu, *Inorg. Chem.*, 2012, **51**, 6577-6591; (c) C. W. Liu, Y.-R. Lin, C.-S. Fang, C. Latouche, S. Kahlal, J.-Y. Saillard, *Inorg. Chem.*, 2013, **52**, 2070-2077; (d) C. Latouche, S. Kahlal, Y.-R. Lin, J.-H. Liao, E. Furet, C. W. Liu, *Inorg. Chem.*, 2013, **52**, 13253-23262; (e) R. S. Dhayal, J.-H. Liao, H.-N. Hou, R. Ervilita, P.-K. Liao, C. W. Liu, *Dalton Trans.*, 2015, **44**, 5898-5908.
- A. J. Edwards, R. S. Dhayal, P.-K. Liao, J.-H. Liao, M.-H. Chiang, R. O. Piltz, S. Kahlal, J.-Y. Saillard, C. W. Liu, *Angew. Chem. Int. Ed.*, 2014, **53**, 7214-7218.
- (a) R. S. Dhayal, J.-H. Liao, Y.-R. Lin, P.-K. Liao, S. Kahlal, J.-Y. Saillard, C. W. Liu, *J. Am. Chem. Soc.*, 2013, **135**, 4704-4707; (b) J.-H. Liao, R. S. Dhayal, X. Wang, S. Kahlal, J.-Y. Saillard, C. W. Liu, *Inorg. Chem.*, 2014, **53**, 11140-11145.
- R. S. Dhayal, J.-H. Liao, X. Wang, Y.-C. Liu, M.-H. Chiang, S. Kahlal, J.-Y. Saillard, C. W. Liu, *Angew. Chem. Int. Ed.*, 2015, **54**, 13604-13608.
- S. K. Barik, S.-C. Huo, C.-Y. Wu, T.-H. Chiu, J.-H. Liao, X. Wang, S. Kahlal, J.-Y. Saillard, C. W. Liu, *Chem. Eur. J.*, DOI: 10.1002/chem.2020001449.
- R. S. Dhayal, J.-H. Liao, S. Kahlal, X. Wang, Y.-C. Liu, M.-H. Chiang, W. E. van Zyl, J.-Y. Saillard, C. W. Liu, *Chem. Eur. J.*, 2015, **21**, 8369-8374.

19. R. P. B. Silalahi, G.-R. Huang, J.-H. Liao, T.-H. Chiu, K. K. Chakrahari, X. Wang, J. Cartron, S. Kahlal, J.-Y. Saillard, C. W. Liu, *Inorg. Chem.*, 2020, **59**, 2536-2547.
20. K. K. Chakrahari, R. P. B. Silalahi, T.-H. Chiu, X. Wang, N. Azrou, S. Kahlal, Y.-C. Liu, M.-H. Chiang, J.-Y. Saillard, C. W. Liu, *Angew. Chem. Int. Ed.*, 2019, **58**, 4943-4947.
21. M. Woinska, S. Grabowsky, P. M. Dominiak, K. Wozniak, D. Jayatilaka, *Sci. Adv.*, 2016, **2**, e1600192.
22. T. H. Lemmen, K. Folting, J. C. Huffman, K. G. Caulton, *J. Am. Chem. Soc.*, 1985, **107**, 7774-7775.
23. BP86/Def2-TZVP level. See SI for computational details.

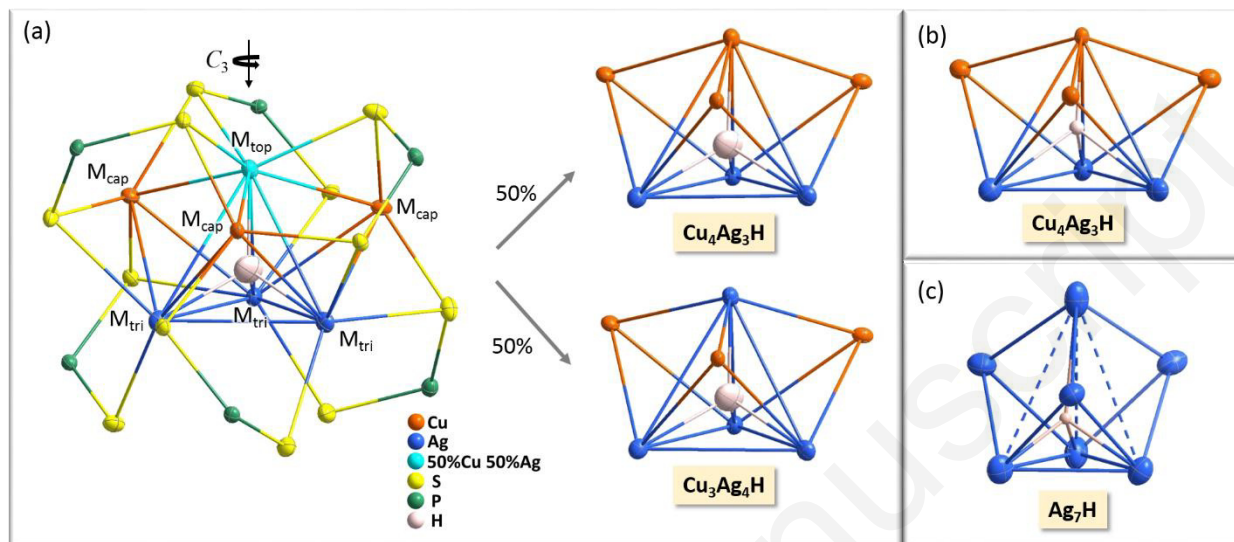


Figure 1. ORTEP drawing (30% probability) of (a) compound **1** (*O*/*Pr* groups omitted). (b) The $\text{Cu}_4\text{Ag}_3\text{H}$ core in **2**, and (c) the Ag_7H core in **3**.

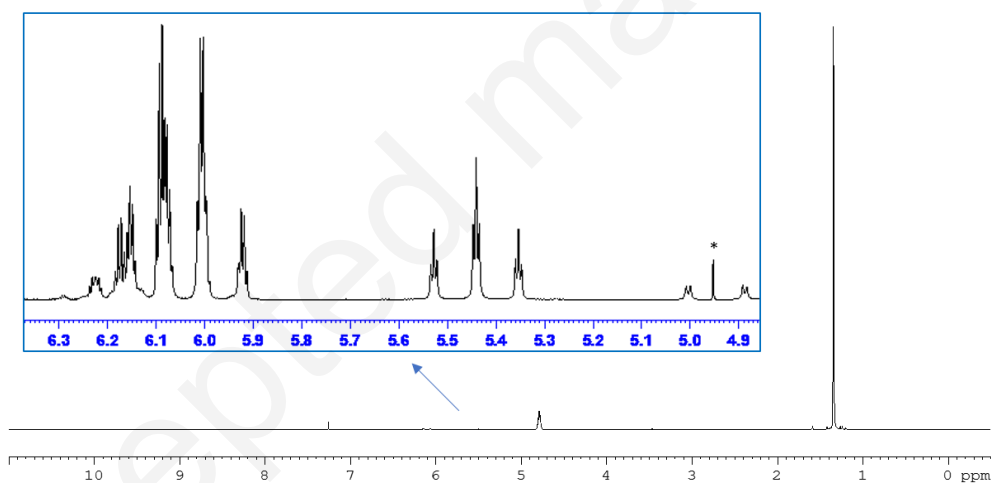


Figure 2. ^1H NMR (800.24MHz, CDCl_3 , r.t.) spectrum of $\text{Cu}_x\text{Ag}_{7-x}(\text{H})\{\text{S}_2\text{P}(\text{O}^i\text{Pr})_2\}_6$. The hydride chemical shift ranges 4.9–6.3 ppm (inset). The asterisk at 4.95 ppm is the resonance of the BHT, which is commonly added in THF solvent as a stabilizer.

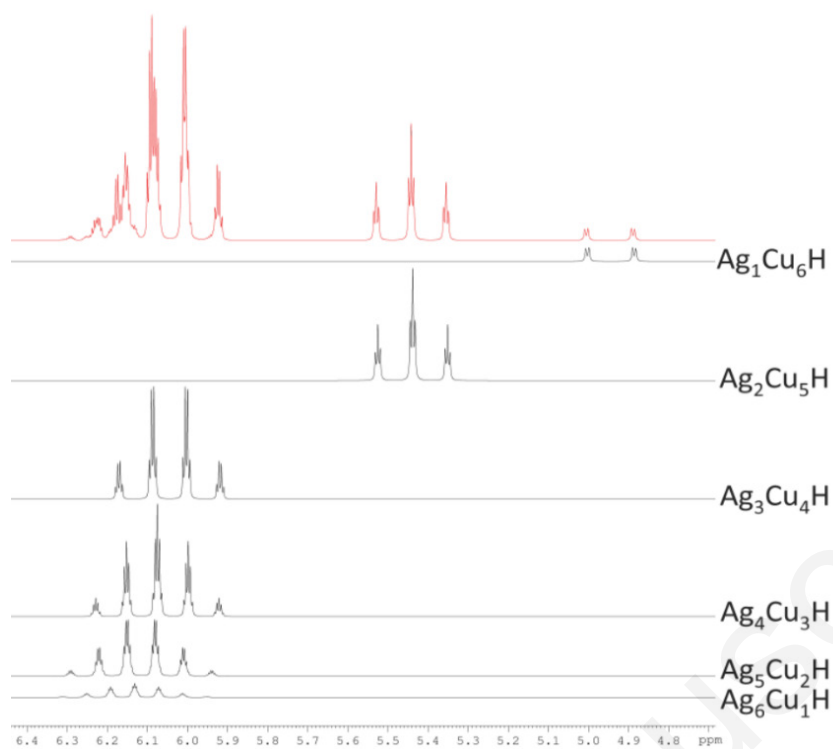


Figure 3. Simulated splitting patterns of a hydride in $\text{Cu}_x\text{Ag}_{7-x}\text{H}$ ($x = 1-6$) in ^1H NMR spectrum. The sum of all simulation is given on the top (red line).

Table 1. The chemical shift and coupling constant of $\text{Cu}_x\text{Ag}_{7-x}(\text{H})\{\text{S}_2\text{P}(\text{O}^i\text{Pr})_2\}_6$, $x = 1-6$ in ^1H and ^{109}Ag NMR spectra.

Cpd.	^1H NMR (ppm)	^1H NMR (ppm) DFT	$^1J(^1\text{H}-^{107}\text{Ag})$ (Hz)	$^1J(^1\text{H}-^{109}\text{Ag})$ (Hz)	Ratio (%)	^{109}Ag NMR (ppm)	$^1J(^1\text{H}-^{109}\text{Ag})$ (Hz)
Cu_6AgH	4.996	5.40	86.7	99.7	2.1	--	--
$\text{Cu}_5\text{Ag}_2\text{H}$	5.441	5.78	65.0	74.7	16.9	1080.5	74.5
$\text{Cu}_4\text{Ag}_3\text{H}$	6.049	5.82	62.9	72.3	40.9	1120.9	72.7
$\text{Cu}_3\text{Ag}_4\text{H}$	6.078	6.45	57.4	66.0	25.1	1140.2	66.6
$\text{Cu}_2\text{Ag}_5\text{H}$	6.116	6.33	52.3	60.1	11.4	1137.4	60.0
CuAg_6H	6.132	6.13	44.6	51.3	3.6	--	--